

Structure and photochromism of Zn(II) thiocyanato complexes of 1-alkyl-2-{{(o-thioalkyl)phenylazo}imidazole}



Shefali Saha (Halder)^a, Chandana Sen^a, Suman Roy^a, Debasish Mallick^{a,1}, Elena López-Torres^b, Chittaranjan Sinha^{a,*}

^a Department of Chemistry, Inorganic Chemistry Section, Jadavpur University, Kolkata 700 032, India

^b Departamento de Química Inorgánica, c/ Francisco Tomás y Valiente, 7, Universidad Autónoma de Madrid, Cantoblanco, 28049 Madrid, Spain

ARTICLE INFO

Article history:

Received 18 March 2015

Accepted 21 May 2015

Available online 28 May 2015

Keywords:

Zn(II)-thioalkylphenyl-azoimidazole

1D chain structure

Photochromism

Activation energy

Rotor mass and volume

ABSTRACT

Zinc(II)-thiocyanato complexes of 1-alkyl-2-{{(o-thioalkyl)phenylazo}imidazole}, $[Zn(SRaaiNR'/(SCN)(\mu-SCN)_2]_n$, are spectroscopically characterized. The single crystal X-ray structure of $[Zn(SMeaaiNEt)(\mu-SCN)(SCN)_2]_n$ shows μ -SCN 1D chain followed by hydrogen bonded 3D supramolecular structure. The UV light irradiation in MeCN solution of the complexes shows E-to-Z (E and Z refer to *trans* and *cis*-configuration about —N=N— , respectively) isomerisation of the coordinated azoimidazole. The rate of isomerisation follows: $[Zn(SEtaaiNET)(SCN)(\mu-SCN)_2] < [Zn(SMeaaiNEt)(SCN)(\mu-SCN)_2] \sim [Zn(SEtaaiNMe)(SCN)(\mu-SCN)_2] < [Zn(SMeaaiNMe)(SCN)(\mu-SCN)_2]$. Quantum yields ($\phi_{E \rightarrow Z}$) and the activation energy (E_a) of the photoisomerisation of the complexes are less than that of free ligand data. This is explained on considering the increase in effective rotor volume of the complexes (complex/rotor volume (cm^3))/E-to-Z isomerisation rate (s^{-1}): $[Zn(SMeaaiNMe)(SCN)_2]/218.515/2.827$; $[Zn(SMeaaiNEt)(SCN)_2]/267.206/2.227$; $[Zn(SEtaaiNMe)(SCN)]/263.399/2.309$; $[Zn(SEtaaiNET)(SCN)]/275.447/1.801$ and hence the lowering of rate of photoisomerisation.

© 2015 Elsevier Ltd. All rights reserved.

1. Introduction

The thiocyanato (SCN^-) and azido (N_3^-) anions are versatile bridging ligands and have synthesized metal complexes of different dimensions [1,2]. Thiocyanato-bridged complexes are involved in a 1,3-coordination mode with the metal ion to produce bridging complexes. The transition metal complexes of $M(\mu-\text{SCN})_nM$ motif exhibits unpredictable magnetic interaction [3]. However, very few μ -thiocyanato complexes show significant structural or magnetic change on stimulation with light [4,5]. In this work we characterize thiocyanato bridging polymer Zn(II) complexes of 1-alkyl-2-{{(o-thioalkyl)phenylazo}imidazole} ($\text{SRaaiNR}'$), $[Zn(SRaaiNR')(\mu-\text{SCN})(SCN)]_n$ and they exhibit optically induced structural changes of coordinated SRaaiNR' about the azo function (—N=N—) without perturbing bridging motif.

Photochromism is a light induced reversible structural change of molecular states who have different absorption spectral characteristics [6]. Organic or hybrid organic-inorganic molecules consisting of photochromic functional motif are useful in the development of optical, storage, recording devices [7].

Arylazoimidazole is a potential switching group in biological applications and in coordination chemistry because of ubiquity of imidazole in biology, especially as a metal coordinating site and in chemistry. This family of compounds has been extensively used as ligands for metal ions by us [8–13] and others [14–16]. We have synthesized 1-alkyl-2-{{(o-thioalkyl)phenylazo}imidazole} ($\text{SRaaiNR}'$), a member of arylazoimidazole family, that has three potential donor centers- N(imidazolyl) (N), N(azo) (N') and thioether (-SR) [17–19]. The ligand, SRaaiNR', can also be bidentate N(imidazolyl) (N), N(azo) (N') chelator [20–22] and monodentate N(imidazolyl) [23] ligand. In this work, we have characterized thiocyanato bridged $[Zn(SRaaiNR')(\mu-\text{SCN})(SCN)]_n$ by single crystal structure elucidation in one case and the complexes have been used to examine the effect of light irradiation in the UV wavelength (Scheme 1). The photophysical properties have been explained by DFT and TD-DFT computation of optimized geometry of a representative complex.

2. Results and discussion

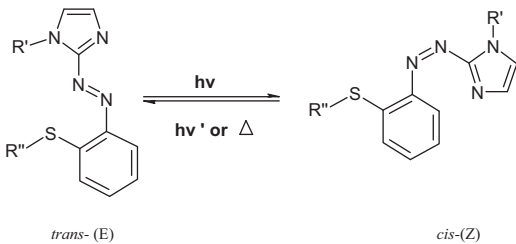
2.1. Synthesis and formulation

o-(Thioalkyl)phenyldiazonium ion is coupled with imidazole in sodium carbonate solution to synthesize

* Corresponding author. Fax: +91 2414 6584.

E-mail address: c_r_sinha@yahoo.com (C. Sinha).

¹ Present address: Department of Chemistry, Mrinalini Datta Mahavidyapith, Kolkata 700 051, India.



Scheme 1. Isomerisation of 1-alkyl-2-(*o*-thioalkyl)phenylazoimidazole.

2-((*o*-thioalkyl)phenylazo)imidazole and has been alkylated by adding alkyl iodide (MeI, EtI) in dry THF solution in presence of NaH to synthesize 1-alkyl-2-((*o*-thioalkyl)phenylazo)imidazole [SRaaiNR' ($R = R' = Me$ (**2a**); $R = Me$, $R' = Et$ (**2b**); $R = Et$, $R' = Me$ (**2c**); $R = R' = Et$ (**2d**)]. The reaction of $Zn(OAc)_2$ with SRaaiNR' in MeOH (1:2 mole proportion) followed by the addition of NH_4SCN (2 equiv.) isolates dark red colored crystalline compounds $[Zn(SRaaiNR')_2(SCN)(\mu-SCN)]_n$ (**3a–3d**). The composition of the complexes has been confirmed by microanalytical data and by other spectroscopic information. The solid state (KBr) IR stretchings at 1622–1625 and 1428–1431 cm^{-1} and are assigned to $\nu(\text{C}=\text{N})$ and $\nu(\text{N}=\text{N})$, respectively [25]. A strong band at 2330–2380 cm^{-1} may be assigned to $\nu(\text{CN})$ of monodentate $-\text{SCN}$ while bridging thiocyanato ($\mu\text{-SCN}$) group shows $\nu(\text{CN})$ at 2050–2150 cm^{-1} . The $\nu(\text{CS})$ is observed at 745–755 cm^{-1} and $\delta(\text{NCS})$ may be assigned to 460–470 cm^{-1} . The ^1H NMR spectra of complexes in CDCl_3 show signals at 7.4 and 7.2 ppm corresponding to imidazolyl 4- and 5-H which have been supported by literature reports [17,24,25]. Phenyl protons (8- to 11-H) of $-\text{S}(\text{R})\text{C}_6\text{H}_4$ remain almost unperturbed. Although single crystal X-ray structure of **3b** (Fig. 1) shows chelated $[\text{Zn}(\text{N(imidazolyl)}, \text{N(azo)})]$ motif of SMeaaiNET but Zn-N(azo) bond length is very long (but less than that of sum of the van der Waals radii of Zn(II) , 1.39 \AA and N(azo) , 1.55 \AA) which might be the reason for not showing significant proton signal movement compared to monodentate Zn-N(imidazolyl) complexes [24] (see Scheme 2).

2.2. Molecular structure of $[\text{Zn}(\text{SMeaaiNET})(\text{SCN})(\mu\text{-SCN})_2]_n$ (**3b**)

The molecular structure of $[\text{Zn}(\text{SMeaaiNET})(\text{SCN})(\mu\text{-SCN})_2]_n$ (**3b**) is shown in Fig. 1. The bond parameters are given in Table 1. The

structure shows pentacoordination about Zn(II) , ZnN_4S sphere. Zn(II) is bridged by $-\text{SCN}-$ groups with two adjacent Zn -centers thus 1-D chain is formed (Fig. 2). The ligand, SMeaaiNET, acts as bidentate $-\text{N(imidazolyl)}, \text{N(azo)}$ chelator. In the bridging unit “[$\text{Zn}(\text{SMeaaiNET})(\mu\text{-SCN})\text{Zn}(\text{SMeaaiNET})$]” two SMeaaiNET show slightly different chelate angles, ‘ $\angle \text{Zn-N(imidazolyl)-N(azo)}$ ’, $\angle \text{N(1)-Zn(1)-N(4)}$, 70.62(1) $^\circ$ and $\angle \text{N(7)-Zn(2)-N(10)}$, 68.26(4) $^\circ$. These angles have been supported by reported data [24–26]. In the polymeric motif the Zn-N(imidazolyl) distances are closely spaced, Zn(1)-N(1) , 1.988(3) and Zn(2)-N(10) , 1.982(3) \AA . The Zn-N(azo) lengths differ slightly in two $\text{Zn}(\text{SMeaaiNET})$ motifs of bridging dimer, $-\text{Zn}(\mu\text{-SCN})_2\text{Zn}-$: Zn(1)-N(4)(azo) , 2.572(4) \AA and Zn(2)-N(10)(azo) , 2.695(2) \AA . The Zn-N(azo) is longer than Zn-N(imidazolyl) which may account the inherent distortion in the geometry and weakening effect of Zn-N(azo) bond. The ZnN_4S is neither the trigonal bipyramidal nor square pyramid; N(1)-N(4)-S(5) forms a distorted trigonal plane (deviation 5.7 $^\circ$). The bridge, $-\text{N}(6)\text{-C}(14)\text{-S}(3)-$ is tilted with trigonal plane, ZnN_2S , by 98.8 $^\circ$ while $-\text{N}(5)\text{-C}(13)\text{-S}(2)-$ bridge makes 111.4 $^\circ$. Bridging motif $-\text{N}(11)\text{-C}(27)\text{-S}(5)-$ makes torsion angle 154.32 $^\circ$ with Zn(1) and 137.58 $^\circ$ with Zn(2) which is in support of significant distortion from linearity. The length of C–N bonds also differ in the bridging and terminal $-\text{SCN}-$: $\text{N}(11)\text{-C}(27)$, 1.150(5) \AA ; $\text{N}(5)\text{-C}(13)$, 1.141(5) \AA ; $\text{N}(6)\text{-C}(14)$, 1.126(5) \AA . The crystal packing shows C–H–S(SCN) recognizable weak interaction and has generated 3D super-build (Fig. 3) network. Thiocyanato-S interacts with imidazolyl-Hs, $\text{C}(9)\text{-H}(9)$ ($\text{C}(9)\text{-H}(9)$ –S(5): $\text{H}(9)$ –S(5), 2.82, $\text{C}(9)$ –S(5), 3.648(4); $\angle \text{C}(9)\text{-H}(9)$ –S(5), 148 $^\circ$ and $\text{C}(23)\text{-H}(23)$ ($\text{C}(23)\text{-H}(23)$ –S(6): $\text{H}(23)$ –S(6), 2.82, $\text{C}(23)$ –S(6), 3.686(5); $\angle \text{C}(9)\text{-H}(9)$ –S(5), 156 $^\circ$; symmetry, $1-x$, $1/2+y$, $1/2-z$) to develop 3D structure. The DFT optimized structure shows metric parameters where bond lengths are elongated by 0.05–0.2 \AA and bond angles are extended by 1–3 $^\circ$ (Supplementary Materials, Table S2).

2.3. UV-Vis spectra and photochromism of $[\text{Zn}(\text{SRaaiNR'})_2(\text{SCN})(\mu\text{-SCN})_2]_n$ (**3a–3d**)

The ligands, SRaaiNR' absorb at 350–360 nm which is assigned to $\pi \rightarrow \pi^*$ transition and weak bands at 420 and 450 nm [17,24,25]. The metal complexes show an additional weak absorption at longer wavelength, 460–465 nm, which is referred to MLCT transition. The TD-DFT and DFT computation of one of the complexes

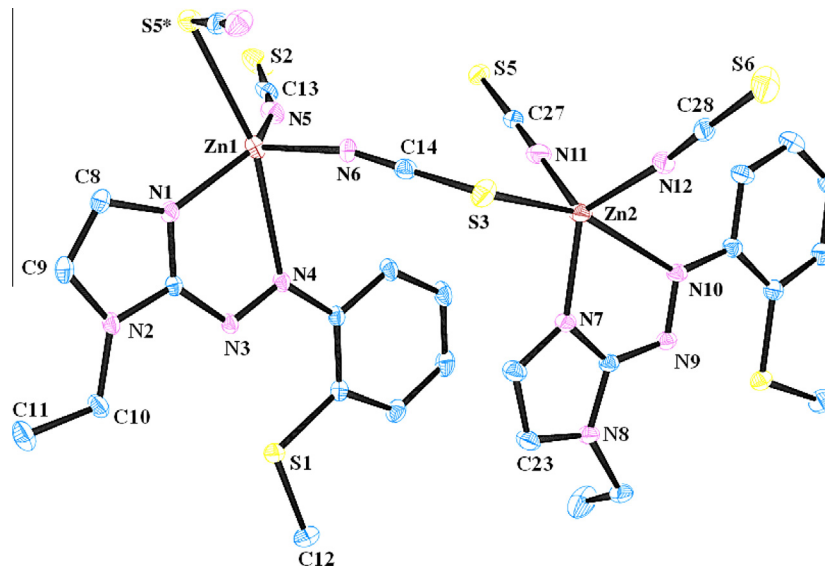
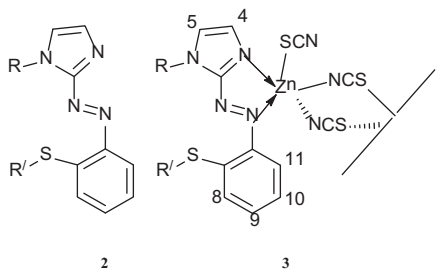


Fig. 1. Crystal structure of $[\text{Zn}(\text{SMeaaiNET})(\mu\text{-SCN})_2]_n$ (**3b**).



[Zn(SRaaiNR')_n(μ-SCN)(SCN)]_n R = R' = Me (**2a/3a**); R = Me, R' = Et (**2b/3b**); R = Et, R' = Me (**2c/3c**); R = R' = Et (**2d/3d**)

Scheme 2. Ligands and the complexes with atom numbering scheme. [Zn(SRaaiNR')_n(μ-SCN)(SCN)]_n R = R' = Me (**2a/3a**); R = Me, R' = Et (**2b/3b**); R = Et, R' = Me (**2c/3c**); R = R' = Et (**2d/3d**).

Table 1
Selected bond distances (Å) and angles (°) for [Zn(SMeaaiEt)(SCN)(μ-SCN)]_n (**3b**).

Bond lengths (Å)			
Zn(1)-N(5)	1.916(4)	Zn(2)-N(12)	1.917(4)
Zn(1)-N(1)	1.988(3)	Zn(2)-N(11)	1.951(4)
Zn(1)-N(6)	1.993(4)	Zn(2)-N(7)	1.982(3)
Zn(1)-S(5)	2.6100(13)	Zn(2)-S(3)	2.5894(15)
Zn(1)-N(4)	2.572(4)	Zn(2)-N(10)	2.695(3)
N(3)-N(4)	1.263(3)	N(9)-N(10)	1.264(2)
Bond angles (°)			
N(5)-Zn(1)-N(1)	127.62(15)	N(12)-Zn(2)-S(3)	93.19(12)
N(5)-Zn(1)-N(6)	114.51(19)	N(11)-Zn(2)-S(3)	103.67(14)
N(1)-Zn(1)-N(6)	114.46(17)	N(7)-Zn(2)-S(3)	96.20(10)
N(5)-Zn(1)-S(5)	94.62(12)	C(14)-S(3)-Zn(2)	103.88(16)
N(1)-Zn(1)-S(5)	93.42(9)	C(27)-S(5)-Zn(1)	95.70(15)
N(6)-Zn(1)-S(5)	100.99(13)	C(7)-N(1)-Zn(1)	119.5(2)
N(12)-Zn(2)-N(11)	113.18(16)	C(8)-N(1)-Zn(1)	135.5(3)
N(12)-Zn(2)-N(7)	126.17(14)	C(7)-N(1)-Zn(1)	119.5(2)
N(11)-Zn(2)-N(7)	115.62(15)	C(8)-N(1)-Zn(1)	135.5(3)
C(22)-N(7)-Zn(2)	131.5(3)	C(13)-N(5)-Zn(1)	165.0(4)
C(27)-N(11)-Zn(2)	176.8(4)	C(14)-N(6)-Zn(1)	161.3(4)
C(28)-N(12)-Zn(2)	166.2(4)	C(21)-N(7)-Zn(2)	122.6(3)
N(1)-Zn(1)-N(4)	70.62(1)	N(7)-Zn(2)-N(10)	68.26(4)

and their molecular functions support the spectral assignment proposal (vide infra). The photoisomerisation of the ligands and the complexes (**Scheme 3**) has been examined in acetonitrile solution (**Figs. 4 and 5**). In solution thiocyanato bridging polymer Zn(II) may be dissociated to solvento species [Zn(SRaaiNR')_n(SCN)₂(Solv)] or nonsolvento [Zn(SRaaiNR')_n(SCN)₂] species who are exhibiting optically induced structural changes. The spectral pattern of the complexes in acetonitrile solution could not draw any logical

conclusion regarding dissociation of thiocyanato bridging polymer to solvent coordinated or solvent free monomer. For clarity, we have used [Zn(SRaaiNR')_n(SCN)₂] monomer for all calculations of photophysical quantitative information. The spectral changes upon light irradiation have been assigned to *trans*-to-*cis* (E-to-Z) isomerisation. The absorption spectra of the E-configuration of coordinated SRaaiNR' in the complexes, **3a–3d**, in acetonitrile are changing with isosbestic point (**Table 2**) upon excitation to the Z-configuration of the ligand. The complexes show little sign of degradation upon repeated irradiation at least up to 15 cycles in each case that has been verified by measuring absorbance before and after irradiation at $\pi \rightarrow \pi^*$ band. The quantum yields were measured for the E-to-Z ($\Phi_{E \rightarrow Z}$) photoisomerisation of these compounds on irradiation of UV wavelength (**Table 2**). The ($\Phi_{E \rightarrow Z}$) values are significantly dependent on the nature of the substituent, halide type and molecular weight [22–28] of the photochrome. The rates of photoisomerisation (*trans*-to-*cis* (E-Z), $\phi_{E \rightarrow Z}$) follows [Zn(SMeaaiNMe)(SCN)₂] (**3a**) > [Zn(SEtaaiNMe)(SCN)₂] (**3b**) ~ [Zn(SMeaaiNEt)(SCN)₂] (**3c**) > [Zn(SEtaaiNEt)(SCN)₂] (**3d**). The observed rate follows the molecular weight sequence of the complexes 411.96 (**3a**), 425.97 (**3b**, **3c**) and 439.99 (**3d**). It helps us to draw a conclusion that photoisomerisation rate is inversely related to molar mass; with increasing molecular weight rates of photoisomerisation decreases.

The thermal Z-to-E (*cis*-to-*trans*) isomerisation of the complexes was examined by UV-Vis spectroscopy (**Fig. 6**) in MeCN at varied temperatures, 302–323 K and the activation energies were obtained (**Table 3**) from Eyring plots (**Fig. 7**). In the complexes the E_{as} are reduced by 34–40% than that of free ligand data which accounts the rate of photoisomerisation. The entropies of activation (ΔS^*) are more negative in the complexes than that of the free ligands. This is also defending the increase in rotor volume in the complexes [27]. DFT optimization of molecular structures of [Zn(SRaaiNR')_n(SCN)₂] and the calculation of rotor volume assigns that the molecule of highest rotor volume ([Zn(SEtaaiNEt)(SCN)₂] rotor volume – 275.447 cm³) shows lowest rate of E → Z light induced isomerisation (1.801 s⁻¹); the rotor volume of [Zn(SRaaiNR')_n(SCN)₂] and rate of E → Z photoisomerisation (s⁻¹) are as follows – [Zn(SMeaaiNMe)(SCN)₂]/218.515 cm³/2.827; [Zn(SMeaaiNEt)(SCN)₂]/267.206 cm³/2.227; [Zn(SEtaaiNMe)(SCN)₂]/263.399 cm³/2.309; [Zn(SEtaaiNEt)(SCN)₂]/275.447 cm³/1.801. Similar complexes of zinc(II)-halides, [Zn(SRaaiNR')X₂(H₂O)] (X = Cl, Br, I) also exhibit molecular weight dependent photochromic rates [25] and the results of present examples support it.

X-ray crystallographic parameters of [Zn(SMeaaiNEt)(SCN)(μ-SCN)₂]_n (**3b**) is used for DFT optimization. The energy difference HOMO/HOMO-1 ($\Delta E_{HOMO/HOMO-1} = 0.15$ eV) is lower than those

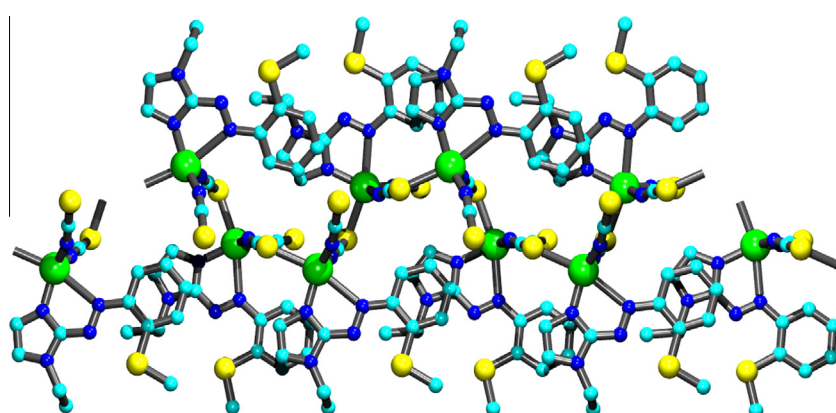


Fig. 2. 1D coordination chain structure of [Zn(SMeaaiNEt)(μ-SCN)₂]_n (**3b**).

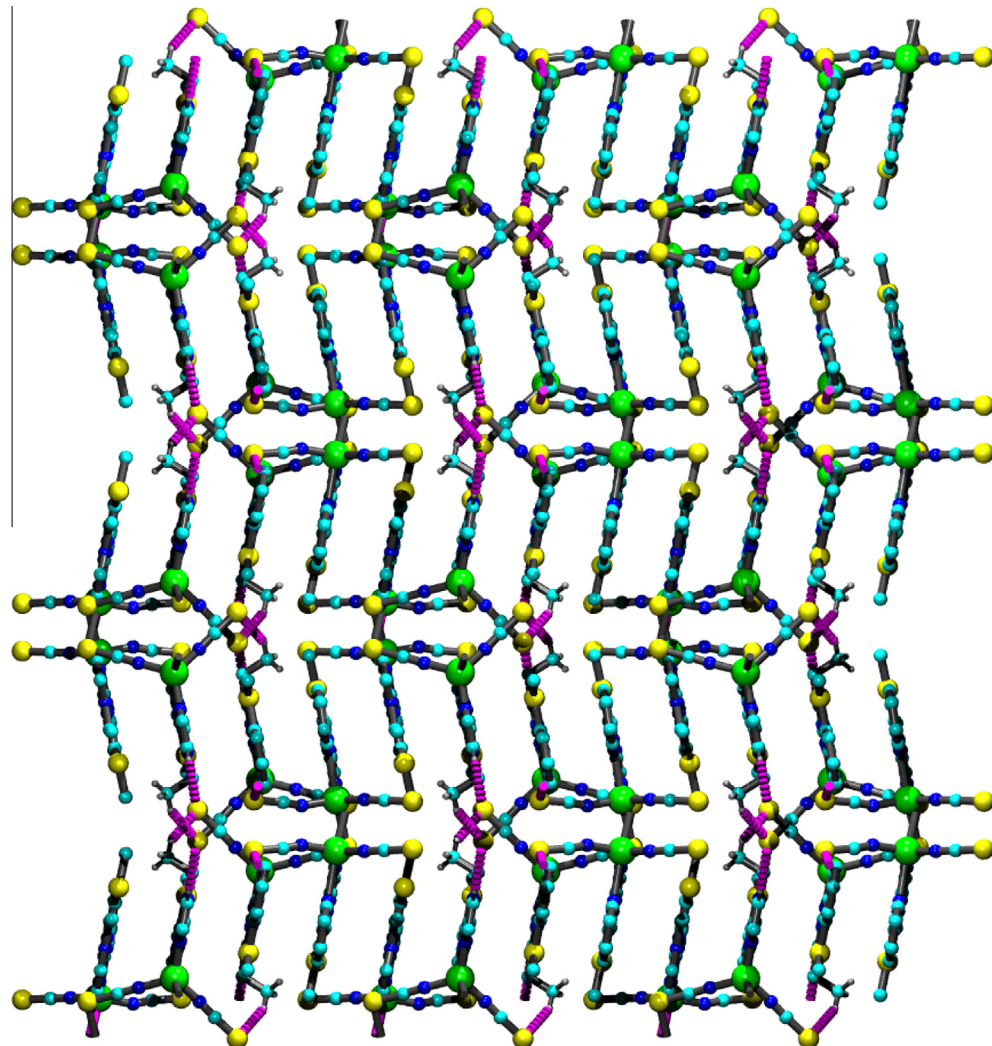
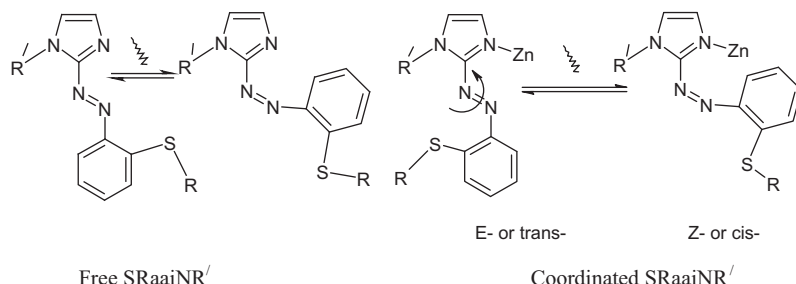


Fig. 3. 3D supramolecular structure of complex $[\text{Zn}(\text{SMeaaiNEm})(\mu\text{-SCN})_2]_n$ (**3b**) formed by hydrogen bonding interactions.

of HOMO-1/HOMO-2 ($\Delta E_{\text{HOMO-1/HOMO-2}} = 0.06 \text{ eV}$). The HOMO contains zinc (Zn) (58%) and thiocyanato ($-\text{SCN}-$) (41%) functions and HOMO-1, HOMO-2 are of exclusively thiocyanato ($-\text{SCN}-$) function type (98%). The LUMO (-4.75 eV) carries Zn (18%) and SCN (82%) while LUMO+1 and LUMO+2 are of SMeaaiNEm (99%) characteristics (Fig. 8). The electronic transitions in the complexes may be associated with intra-ligand $\pi(\text{azoimine}) \rightarrow \pi^*(\text{azoimine})$, interligand $\pi(\text{SCN}) \rightarrow \pi^*(\text{azoimine})$ and $d\pi(\text{Zn}) \rightarrow \pi^*(\text{SCN, azoimine})$ charge transfer transitions. The useful calculated transitions are HOMO-13 \rightarrow LUMO+1 (372 nm), HOMO-9 \rightarrow LUMO (440 nm)/LUMO+1 (432 nm) and have been assigned to intraligand

charge transfer transitions associated with $\pi(\text{azoimine}) \rightarrow \pi^*(\text{azoimine})$ [22–26]. The metal-to-ligand charge transfer characters are observed with HOMO \rightarrow LUMO+1 while HOMO-1/HOMO-2 \rightarrow LUMO+1/LUMO+2 have been assigned to $\pi(\text{thiocyanato}) \rightarrow \pi^*(\text{azoimine})$ at 460 nm. The observed spectrum of the complex shows the transitions at 358, 420 and 465 nm and thus supports the calculated transitions.

The UV light irradiation ($<360 \text{ nm}$) may cause $\pi \rightarrow \pi^*$ transition followed by E-to-Z transformation of coordinated Raai-C_nH_{2n+1}. The irradiation is carried out for a fixed time which will enforce to isomerize more stable *trans*-isomer to *cis*-isomer. The MLCT or



Scheme 3. Photochromism of free and coordinated SRaaiNR[/].

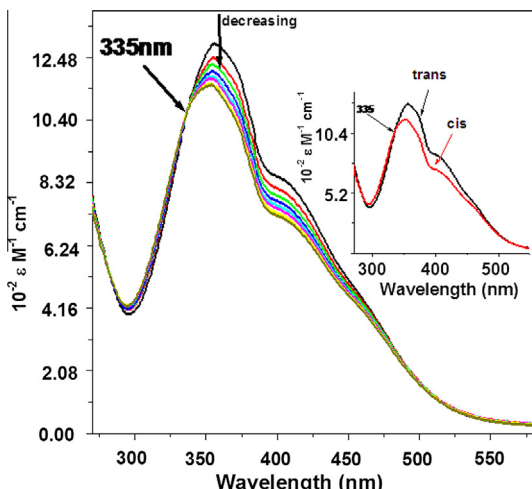


Fig. 4. Spectral changes due to E → Z isomerisation of SEtaaiNET in MeCN upon repeated irradiation at 357 nm at 3 min interval at 25 °C.

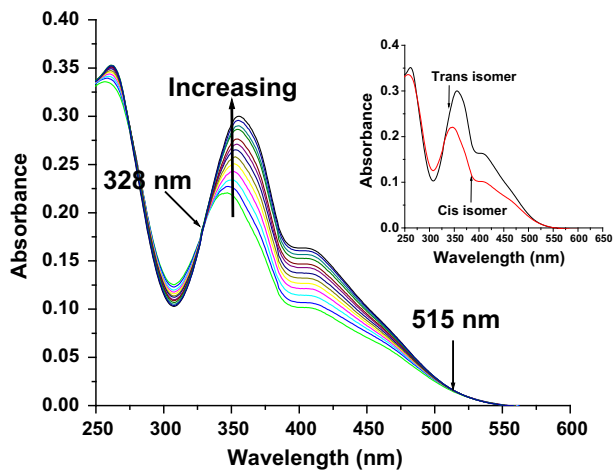


Fig. 5. Spectral changes of E → Z isomerisation of coordinated SEtaaiNET at $[Zn(SMeaaaiNET)(SCN)(\mu-SCN)]_2$ (3b) in MeCN upon repeated irradiation at 359 nm at 3 min interval at 25 °C.

inter-ligand XLCT are of lower energetic transitions (even lower than intraligand $\pi-\pi^*$) which may not capable to perform physical process like isomerisation. Conversely, the ligand in the complexes may assist charge transition in a secondary (MLCT or XLCT) process which is responsible for deactivation of excited species and regulates the rate of isomerisation and quantum yields.

3. Experimental

3.1. Materials

Zn(OAc)₂ is obtained from E-Merck, India. 1-Alkyl-2-{(o-thioalkyl)phenyl azo}imidazole were synthesized by reported procedure [17]. All other chemicals and solvents were reagent grade as received.

3.2. Physical measurements

Microanalytical data (C, H, N) were collected on Perkin-Elmer 2400 CHNS/O elemental analyzer. Spectroscopic data were collected using the following instruments: UV-Vis spectra from a Perkin Elmer Lambda 25 spectrophotometer; IR spectra (KBr disk, 4000–2000 cm^{-1}) from a Perkin Elmer RX-1 FTIR spectrophotometer; photoexcitation has been carried out using a Perkin Elmer LS-55 spectrofluorimeter and ¹H NMR spectra from a Bruker (AC) 300 MHz FTNMR spectrometer.

3.3. Preparation of compounds

3.3.1. $[Zn(SMeaaaiNET)(SCN)(\mu-SCN)]_2$ (3b)

1-Ethyl-2-{(o-thiomethyl)phenyl azo}imidazole (33.75 mg, 0.14 mmol) in CH₃OH was added in drops to MeOH solution of Zn(OAc)₂ (30 mg, 0.14 mmol) and H₂O-MeOH solution of NH₄SCN (20.80 mg, 0.27 mmol) was added in drops to it and was stirred for 2 h. The resultant reddish solution was collected by filtration; slow evaporation of the solution gives the red crystal. The yield was 38.05 mg (65%). Other complexes were prepared under identical conditions from H₂O-MeOH solution and the yield varied in the range 60–70%.

Microanalytical data of the complexes are as follows: $[Zn(SMeaaaiNMe)(SCN)(\mu-SCN)]_2$ (3a) *Anal.* Calc. for $[ZnC_{13}H_{12}N_6S_3]$: C, 37.77; H, 2.92; N, 20.31. Found: C, 37.69; H, 2.89; N, 20.35%. FT-IR (KBr disc, cm^{-1}), $\nu(\text{N}=\text{N})$, 1430; $\nu(\text{C}=\text{N})$, 1623; $\nu(\text{SCN})$, 2135–2140, 2075–2080 cm^{-1} . UV-VIS spectroscopic data in CH₃CN ($\lambda_{\max}(\text{nm})(10^{-3} \epsilon (\text{dm}^3 \text{mol}^{-1} \text{cm}^{-1}))$): 357 (15.92), 422 (8.37), 463 (8.60). ¹H NMR (CDCl₃; δ , ppm): 7.44 (bs, 4-H), 7.41 (bs, 5-H), 7.47 (8-H, d, $J = 8.00 \text{ Hz}$), 7.55 (9-H, m), 8.28 (11-H, d, 8.00 Hz), 2.43 (s, S-CH₃). $[Zn(SEtaaiNMe)(SCN)(\mu-SCN)]_2$ (3b) *Anal.* Calc. for $[ZnC_{14}H_{14}N_6S_3]$: C, 39.30; H, 3.30; N, 19.64. Found: C, 39.36; H, 3.23; N, 19.59%. FT-IR (KBr disc, cm^{-1}), $\nu(\text{N}=\text{N})$, 1428; $\nu(\text{C}=\text{N})$, 1624; $\nu(\text{SCN})$, 2138–2140, 2070–2080 cm^{-1} . UV-VIS spectroscopic data in CH₃CN ($\lambda_{\max}(\text{nm})(10^{-3} \epsilon (\text{dm}^3 \text{mol}^{-1} \text{cm}^{-1}))$): 359 (18.99), 422 (10.52), 467 (8.81). ¹H NMR (CDCl₃; δ , ppm): 7.44 (bs, 4-H), 7.45 (bs, 5-H), 7.48 (8-H, d, $J = 8.00 \text{ Hz}$), 7.60 (9-H, m), 8.30 (11-H, d, 8.34 Hz), 4.36 (q, N(1)-CH₂, $J = 7.29 \text{ Hz}$), 1.42 (t, (N(1)-CH₂)-CH₃, $J = 7.27 \text{ Hz}$), 2.44 (2, -S-CH₃). $[Zn(SMeaaaiNET)(SCN)(\mu-SCN)]_2$ (3c) *Anal.* Calc. for $[ZnC_{14}H_{14}N_6S_3]$: C, 39.30; H, 3.30; N, 19.64. Found: C, 39.34; H,

Table 2

Excitation wavelength (λ_{π, π^*}), rate of (E) trans (t) → (Z) cis (c) conversion and quantum yield ($\phi_{t \rightarrow c}$) in MeCN.

Compound	λ_{π, π^*} (nm)	Isobestic points (nm)	Rate of E → Z conversion $\times 10^8$ (s^{-1})	($\Phi_{E \rightarrow Z}$)
SMeaaaiNMe (2a) ^a	357	337	4.908	0.317
SMeaaaiNET (2b) ^a	358	337	3.108	0.232
SEtaaiNMe (2c) ^a	357	336	4.670	0.290
SEtaaiNET (2d) ^a	356	335	2.948	0.197
$[Zn(SMeaaaiNMe)(SCN)(\mu-SCN)]_2$ (3a)	357	335	2.827	0.142
$[Zn(SMeaaaiNET)(SCN)(\mu-SCN)]_2$ (3b)	359	334	2.227	0.125
$[Zn(SEtaaiNMe)(SCN)(\mu-SCN)]_2$ (3c)	358	335	2.309	0.130
$[Zn(SEtaaiNET)(SCN)(\mu-SCN)]_2$ (3d)	359	334	1.801	0.090

^a Data are obtained from Ref. [25].

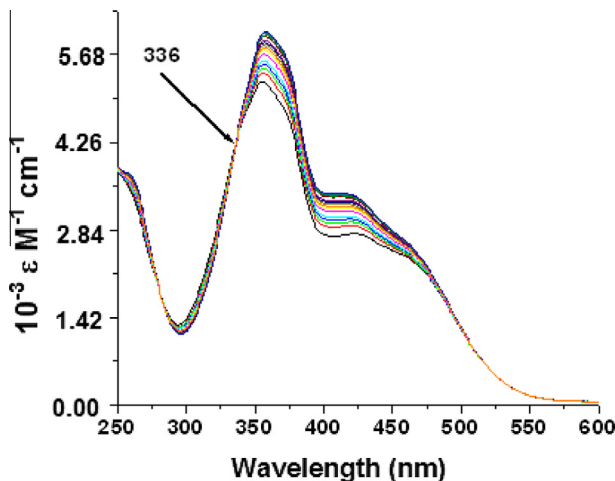


Fig. 6. Spectral changes during $Z \rightarrow E$ isomerisation of $[Zn(SMeaaiNMe)(SCN)(\mu\text{-}SCN)_2]_n$ (**3b**) in MeCN solution at 298 K. Z-isomer is generated by irradiation of UV light for 45 min.

3.26; N, 19.67%. FT-IR (KBr disc, cm^{-1}), $\nu(\text{N}=\text{N})$, 1431; $\nu(\text{C}=\text{N})$, 1625; $\nu(\text{SCN})$, 2140–2145, 2075–2078 cm^{-1} . UV-VIS spectroscopic data in CH_3CN ($\lambda_{\text{max}}(\text{nm})(10^{-3} \epsilon (\text{dm}^3 \text{mol}^{-1} \text{cm}^{-1}))$): 358(17.6), 420 (9.77), 465 (8.58). ^1H NMR (CDCl_3 ; δ , ppm): 7.48 (bs, 4-H), 7.44 (bs, 5-H), 7.42 (8-H, d, $J = 8.00 \text{ Hz}$), 7.50 (9-H, m), 8.10 (11-H, d, 8.00 Hz), 4.18 (s, N(1)- CH_3), 3.19 (q, - $\text{S}-\text{CH}_2$, $J = 7.28 \text{ Hz}$), 1.38 (t, - $\text{S}-\text{CH}_3$, $J = 7.25 \text{ Hz}$). $[Zn(SEtaaiNMe)(SCN)(\mu\text{-}SCN)_2]_n$ (**3d**) Anal. Calc. for $[\text{ZnC}_{14}\text{H}_{14}\text{N}_6\text{S}_3]$: C, 40.77; H, 3.65; N, 19.05. Found: C, 40.70; H, 3.68; N, 19.07%. FT-IR (KBr disc, cm^{-1}), $\nu(\text{N}=\text{N})$, 1429; $\nu(\text{C}=\text{N})$, 1622; $\nu(\text{SCN})$, 2135–2145, 2080–2090 cm^{-1} . UV-VIS spectroscopic data in CH_3CN ($\lambda_{\text{max}}(\text{nm})(10^{-3} \epsilon$

($\text{dm}^3 \text{mol}^{-1} \text{cm}^{-1})$): 359 (16.99), 421 (11.22), 461 (9.01). ^1H NMR (CDCl_3 ; δ , ppm): 7.48 (bs, 4-H), 7.47 (bs, 5-H), 7.41 (8-H, d, $J = 8.00 \text{ Hz}$), 7.49 (9-H, m), 8.00 (11-H, d, 8.00 Hz), 4.32 (q, N(1)- CH_2 , $J = 7.28 \text{ Hz}$), 1.42 (2, - $\text{S}-\text{CH}_3$, $J = 7.28 \text{ Hz}$), 3.19 (q, - $\text{S}-\text{CH}_2$, $J = 7.29 \text{ Hz}$), 1.39 (t, - $\text{S}-\text{CH}_3$, $J = 7.27 \text{ Hz}$).

3.4. X-ray diffraction study

Single crystals of $[Zn(SEtaaiNMe)(SCN)(\mu\text{-}SCN)_2]_n$ (**3b**) suitable for data collection were grown from slow evaporation of H_2O -MeOH solution of the complexes. The crystal data and details of the data collections are given in Table 4. Suitable single crystal of the complex **3b** ($0.20 \times 0.20 \times 0.10 \text{ mm}$) was mounted on a Bruker SMART APEX CCD diffractometer (graphite monochromated Mo $K\alpha$ radiation, $\lambda = 0.71073 \text{ \AA}$) and data were collected by use of ω scans. Unit cell parameters were determined from least-squares refinement of setting angles (θ) within the range $1.72 \leq \theta \leq 27.67$ (**3b**). Data were corrected for Lorentz polarization effects and for linear decay with in hkl range $-19 \leq h \leq 19$, $-25 \leq k \leq 26$, $-16 \leq l \leq 16$. Semi-empirical absorption corrections based on ψ -scans were applied. The structures were solved by direct method using SHELXS-97 [29] and successive difference Fourier synthesis. All non-hydrogen atoms were refined anisotropically. The hydrogen atoms were fixed geometrically and refined using the riding model. The maximum and minimum residual electron densities were 1.111 and $-0.528 \text{ e \AA}^{-3}$. All calculation was carried out using SHELXS-97 [30], ORTEP-32 [31] and PLATON-99 [32] programs.

3.5. Photometric measurements

Absorption spectra were taken with a PerkinElmer Lambda 25 UV/Vis Spectrophotometer in a $1 \times 1 \text{ cm}$ quartz optical cell maintained at 25°C with a Peltier thermostat. The light source of a

Table 3
Rate and activation parameters for Z (c) \rightarrow (E) *trans* (t) thermal isomerisation.

Compound	Temp. (K)	Rate of thermal $Z \rightarrow E$ conversion $\times 10^4$ (s^{-1})	E_a , kJ mol^{-1}	ΔH^* , kJ mol^{-1}	ΔS^* , $\text{J mol}^{-1} \text{K}^{-1}$	ΔG^* , kJ mol^{-1}
SMeaaiNMe (2a) ^a	298	4.329	25.42	22.88	-232.41	93.87
	303	5.295				
	308	6.191				
	313	7.091				
	313	7.269				
SMeaaiNEt (2b) ^a	298	4.614	22.99	20.45	-240.02	93.77
	303	5.598				
	308	6.293				
	313	7.269				
	313	7.269				
SEtaaiNMe (2c) ^a	298	4.425	21.92	19.38	-244.04	93.94
	303	5.123				
	308	5.985				
	313	6.729				
	313	6.589				
SEtaaiNEt (2d) ^a	298	4.625	18.88	16.34	-253.96	93.93
	303	5.123				
	308	5.985				
	313	6.589				
	313	6.589				
(3a)	302	6.274	16.84	14.240	-259.20	81.02
	309	7.233				
	316	8.433				
	323	9.677				
	323	9.677				
(3b)	302	6.655	14.92	12.32	-265.16	82.47
	309	7.302				
	316	8.512				
	323	9.721				
	323	9.721				
(3c)	302	6.730	14.55	11.95	-266.28	83.23
	309	7.395				
	316	8.550				
	323	9.752				
	323	9.752				
(3d)	302	7.101	11.34	8.745	-276.47	83.41
	309	7.612				
	316	8.380				
	323	9.540				

^a Data are obtained from Ref. [25].

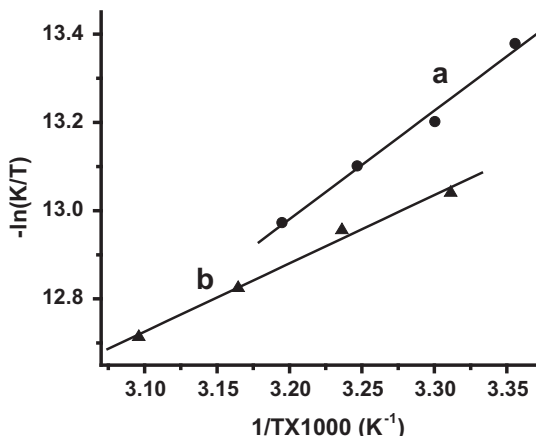


Fig. 7. The Eyring plots of rate constants of Z-to-E thermal isomerisation of SMeaaiNET (**a**) and $[Zn(SMeaaiNET)(SCN)(\mu\text{-}SCN)_2]_n$ (**3b**) (**b**) at different temperatures.

PerkinElmer LS 55 spectrofluorimeter was used as an excitation light, with a slit width of 10 nm. An optical filter was used to cut off overtones when necessary. Upon UV light irradiation at λ_{\max} of the $\pi\text{-}\pi^*$ absorption to a solution of the complex, the intense peak decreases, which is accompanied by a slight increase at the tail portion of the spectrum around 450 nm ($n\text{-}\pi^*$) until a Photostationary state (PSS-I) is reached. Subsequent irradiation at the newly appeared longer wavelength peak reverses the course of the reaction and the original spectrum is recovered up to a point, which is another Photostationary state (PSS-II) under $n\pi^*$ irradiation. An isosbestic point at 335–340 nm is reached during this process. The absorption spectra of the *cis*-isomers of all the complexes were obtained by extrapolation of the absorption spectra of a *cis*-rich mixture for which the composition is known from 1H NMR integration. Quantum yields (ϕ) were obtained by

Table 4
Crystallographic data for $[Zn(SMeaaiNET)(SCN)(\mu\text{-}SCN)_2]$ (**3b**).

	3b
Empirical formula	C ₁₄ H ₁₄ N ₆ S ₃ Zn
Formula weight	427.86
T (K)	293(2)
Crystal system	monoclinic
Space group	P ₂ 1/n
Crystal size (mm)	0.20 × 0.20 × 0.10
Unit cell dimensions	
<i>a</i> (Å)	14.8468(4)
<i>b</i> (Å)	19.9903(5)
<i>c</i> (Å)	12.4978(5)
β (°)	97.103(2)
<i>V</i> (Å) ³	3680.8(2)
<i>Z</i>	8
λ (Å)	0.71073
μ (Mo K α) (mm ⁻¹)	1.683
<i>D</i> _{calc} (mg m ⁻³)	1.544
θ range (°)	1.72–27.67
Refine parameters	433
Total reflection	8499
Unique data [$I > 2\sigma(I)$]	5042
R_1 ^a [$I > 2\sigma(I)$]	0.0534
wR_2 ^b	0.1279
Goodness of fit (GOF)	1.017

^a $R = \sum|F_o - F_c|/\sum F_o$.

^b $wR = [\sum w(F_o^2 - F_c^2)/\sum wF_o^4]^{1/2}$ are general but *w* are different, *w* = 1/[$\sum(F_o^2) + (0.0665P)^2 + 2.1925P$] for (**3b**) where *P* = ($F_o^2 + 2F_c^2$)/3.

measuring initial E-to-Z isomerisation rates (v) in a well-stirred solution within the above instrument using the equation,

$$v = (\phi I_0/V)(1 - 10^{-\text{Abs}})$$

where I_0 is the photon flux at the front of the cell, V is the volume of the solution, and Abs is the initial absorbance at the irradiation wavelength. The value of I_0 was obtained by using azobenzene ($\phi = 0.11$ for $\pi\text{-}\pi^*$ excitation [33]) under the same irradiation conditions.

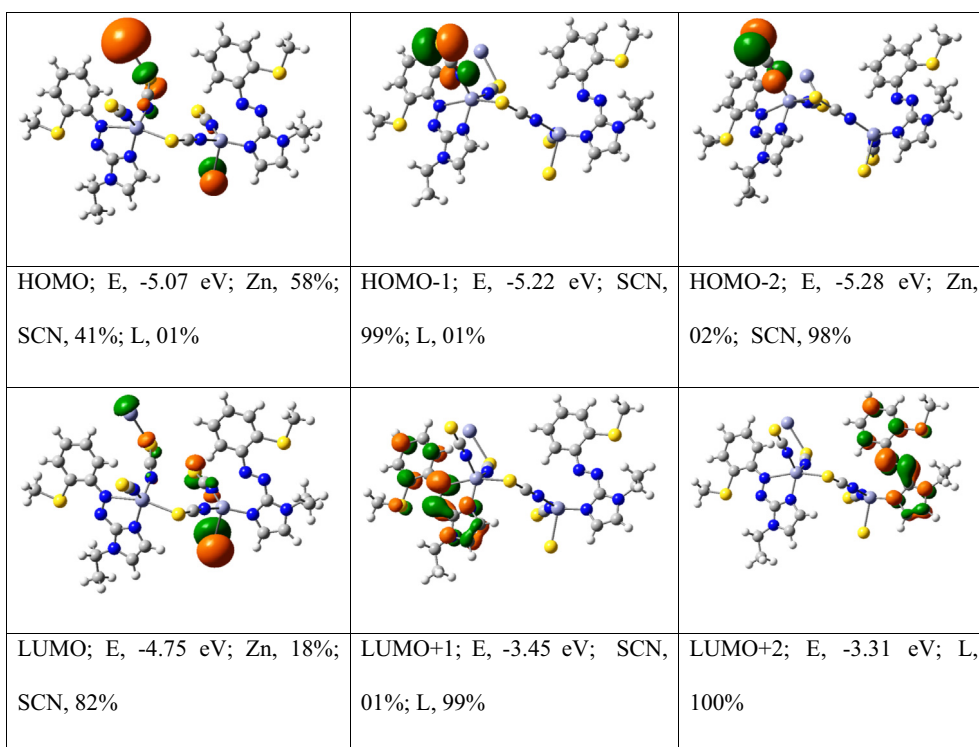


Fig. 8. Surface plots of molecular orbitals of motif “[SMeaaiNET]Zn(μ -SCN)Zn(SMeaaiNET)” including their composition and energy.

The thermal rates of Z-to-E isomerisation were obtained by monitoring absorption changes intermittently for a *cis*-rich solution kept in the dark at constant temperatures (T) in the range from 298–321 K. The activation energy (E_a) and the frequency factor (A) were obtained from the Arrhenius plot, $\ln k = \ln A - E_a/RT$, where k is the measured rate constant, R is the gas constant, and T is temperature. The values of activation free energy (ΔG^*) and activation entropy (ΔS^*) were obtained through the relationships, $\Delta G^* = E_a - RT - T\Delta S^*$ and $\Phi_{E-Z} = \Delta S^* = \ln A - 1 - \ln(k_B T/h)/R$, where k_B and h are Boltzmann's and Plank's constants.

3.6. Computational study

All calculations were executed by using Gaussian09 program software package [34]. Full geometry optimizations were carried out using the density functional theory method at the B3LYP level [35,36] for the representative complex, $[Zn(SMeaaiNEt)(SCN)(\mu-SCN)_2]_n$ (**3b**). The calculations were performed by using monomer motif of bridging polymer. The lanL2DZ effective potential (ECP) set of Hay and Wadt [37,38] for Zn and S atoms and the standard 6-31 + G(d) basis set for C, H, and N atoms were used in the calculations. The vibrational frequency calculations were performed to ensure that the optimized geometries represent the local minima and there are only positive eigen values. Vertical electronic excitations based on B3LYP optimized geometries were computed using the time-dependent density functional theory (TDDFT) formalism in acetonitrile using conductor-like polarizable continuum model (CPCM) [39–41] using the same B3LYP level and basis sets. GAUSSSUM was used to calculate the fractional contributions of various groups to each molecular orbital.

4. Conclusion

$[Zn(SRaaiNR)(SCN)(\mu-SCN)_2]_n$ ($SRaaiNR^f$, 1-alkyl-2-((*o*-thioalkyl)phenylazo)imidazoles) are structurally characterized by different spectroscopic data. The structural confirmation by single crystal X-ray diffraction measurement shows the bidentate chelation of $SRaaiNR^f$ and bridging –SCN– groups. Photochromism of the complexes are examined by UV light irradiation in MeCN solution and the results are compared with free ligand data and those of $[Zn(SRaaiNR)X_2(H_2O)]$ [25]. Quantum yields of E-to-Z isomerisation are determined in MeCN for ligands and complexes. The Z-to-E isomerisation is thermally driven process. The activation energy (E_a) of Z-to-E isomerisation has been influenced by the molar volume of the complexes.

Acknowledgments

Financial support from West Bengal DST (228/1(10)/(Sanc.)/ST/P/S&T/9G-16/2012), Kolkata and University Grants Commission (F.42-333/2013(SR)), New Delhi are gratefully acknowledged.

Appendix A. Supplementary data

CCDC 1052335 contain the supplementary crystallographic data for the structure of $[Zn(SMeaaiNEt)(SCN)(SCN)]_n$ (**3b**). These data can be obtained free of charge via <http://www.ccdc.cam.ac.uk/conts/retrieving.html>, or from the Cambridge Crystallographic Data Centre, 12 Union Road, Cambridge CB2 1EZ, UK; fax: (+44)

1223 336 033; or e-mail: deposit@ccdc.cam.ac.uk. Supplementary data associated with this article can be found, in the online version, at <http://dx.doi.org/10.1016/j.poly.2015.05.031>.

References

- [1] A.M. Golub, H. Kohler, V.V. Skopenko (Eds.), *Chemistry of Pseudohalides*, Elsevier, Amsterdam, 1986.
- [2] S.T. Hyde, B. Ninham, S. Anderson, Z. Blum, T. Landh, K. Larsson, S. Liddin, *The Language of Shape*, Elsevier, Amsterdam, 1997.
- [3] S. Chattopadhyay, M.G.B. Drew, C. Diaz, A. Ghosh, *Dalton Trans.* (2007) 2492.
- [4] X.Q. Wang, W.T. Yu, D. Xu, M.K. Lu, D.R. Yuan, *Acta Crystallogr. C* 56 (2000) 418.
- [5] X.Q. Wang, D. Xu, M.K. Lu, D.R. Yuan, S.X. Xu, *Mater. Res. Bull.* 36 (2001) 879.
- [6] G.H. Brown (Ed.), *Photochromism*, Wiley-Interscience, New York, 1971.
- [7] H. Durr, H. Bouas-Laurent (Eds.), *Photochromism, Molecules and Systems*, Elsevier, Amsterdam, 1990.
- [8] D. Sardar, P. Datta, S. Das, C.-D. Chen, C.-J. Chen, B. Saha, S. Samanta, D. Bhattacharjee, P. Karmakar, C. Sinha, *Inorg. Chim. Acta* 394 (2013) 98.
- [9] D. Sardar, P. Datta, P. Mitra, C. Sinha, *Polyhedron* 29 (2010) 3170.
- [10] P. Bhunia, U.S. Ray, J. Cheng, T.-H. Lu, C. Sinha, *Polyhedron* 27 (2008) 3191.
- [11] P. Datta, D. Sardar, P. Mitra, C. Sinha, *Polyhedron* 30 (2011) 1516.
- [12] S.K. Sarkar, M.S. Jana, T.K. Mondal, C. Sinha, *J. Organomet. Chem.* 716 (2012) 129.
- [13] S.K. Sarkar, M.S. Jana, T.K. Mondal, C. Sinha, *Appl. Organometal. Chem.* 28 (2014) 641.
- [14] A. Pramanik, S. Majumdar, G. Das, *CrystEngComm* 12 (2010) 250.
- [15] A. Pramanik, G. Das, *Polyhedron* 29 (2010) 2999.
- [16] J.A.F. Gamelas, A.M.V. Cavaleiro, E. vina de, M. Gomes, M. Belsley, E. Herdtweck, *Polyhedron* 21 (2002) 2537.
- [17] D. Banerjee, U. Ray, S.K. Jasimuddin, J.-C. Liou, T.-H. Lu, C. Sinha, *Polyhedron* 25 (2006) 1299.
- [18] T.K. Mondal, P. Raghavaiah, A.K. Patra, C. Sinha, *Inorg. Chem. Commun.* 13 (2010) 273.
- [19] S. Nandi, D. Bannerjee, P. Datta, T.-H. Lu, A.M.Z. Slawin, C. Sinha, *Polyhedron* 28 (2009) 3519.
- [20] P. Bhunia, D. Bannerjee, P. Datta, P. Raghavaiah, A.M.Z. Slawin, J.D. Woollins, J. Ribas, C. Sinha, *Eur. J. Inorg. Chem.* (2010) 311.
- [21] K.K. Sarker, S. Saha Halder, D. Banerjee, T.K. Mondal, A.R. Paital, P.K. Nanda, P. Raghavaiah, C. Sinha, *Inorg. Chim. Acta* 363 (2010) 2955.
- [22] T.K. Mondal, J.-S. Wu, T.-H. Lu, S.K. Jasimuddin, C. Sinha, *J. Organomet. Chem.* 694 (2009) 3518.
- [23] S. Saha (Halder), P. Raghavaiah, C. Sinha, *Polyhedron* 46 (2012) 25.
- [24] S. Saha (Halder), B.G. Chand, J.-S. Wu, T.-H. Lu, P. Raghavaiah, C. Sinha, *Polyhedron* 46 (2012) 81.
- [25] P. Dutta, D. Mallick, S. Roy, E.L. Torres, C. Sinha, *Inorg. Chim. Acta* 423 (2014) 397.
- [26] S. Saha (Halder), P. Mitra, C. Sinha, *Polyhedron* 67 (2014) 321.
- [27] S. Saha (Halder), S. Roy, T.K. Mondal, R. Saha, C. Sinha, *Z. Anorg. Alleg. Chem.* 639 (2013) 1861.
- [28] Y. Lee, M. Lee, *J. Phys. Chem. A* 117 (2013) 12878.
- [29] H. Nishihara, *Bull. Chem. Soc. Jpn.* 77 (2004) 407.
- [30] G.M. Sheldrick, *SHELXS-97*, University of Gottingen, Germany, 1997.
- [31] G.M. Sheldrick, *SHELXS-97*, University of Gottingen, Germany, 1997.
- [32] J. Farrugia, *ORTEP-3 for windows*, *J. Appl. Crystallogr.* 30 (1997) 565.
- [33] A.L. Spek, PLATON, The Netherlands (1999).
- [34] G. Zimmerman, L. Chow, U. Paik, *J. Am. Chem. Soc.* 80 (1958) 3528.
- [35] M.J. Frisch, G.W. Trucks, H.B. Schlegel, G.E. Scuseria, M.A. Robb, J.R. Cheeseman, G. Scalmani, V. Barone, B. Mennucci, G.A. Petersson, H. Nakatsuji, M. Caricato, X. Li, H.P. Hratchian, A.F. Izmaylov, J. Bloino, G. Zheng, J.L. Sonnenberg, M. Hada, M. Ehara, K. Toyota, R. Fukuda, J. Hasegawa, M. Ishida, T. Nakajima, Y. Honda, O. Kitao, H. Nakai, T. Vreven, J.A. Montgomery Jr., J.E. Peralta, F. Ogliaro, M. Bearpark, J.J. Heyd, E. Brothers, K.N. Kudin, V.N. Staroverov, R. Kobayashi, J. Normand, K. Raghavachari, A. Rendell, J.C. Burant, S.S. Iyengar, J. Tomasi, M. Cossi, N. Rega, M.J. Millam, M. Klene, J.E. Knox, J.B. Cross, V. Bakken, C. Adamo, J. Jaramillo, R. Gomperts, R.E. Stratmann, O. Yazyev, A.J. Austin, R. Cammi, C. Pomelli, J.W. Ochterski, R.L. Martin, K. Morokuma, V.G. Zakrzewski, G.A. Voth, P. Salvador, J.J. Dannenberg, S. Dapprich, A.D. Daniels, Ö. Farkas, J.B. Foresman, J.V. Ortiz, J. Cioslowski, D.J. Fox, *GAUSSIAN 09*, Revision D.01, Gaussian Inc., Wallingford, CT, (2009).
- [36] A.D. Becke, *J. Chem. Phys.* 98 (1993) 5648.
- [37] C. Lee, W. Yang, R.G. Parr, *Phys. Rev. B* 37 (1988) 785.
- [38] P.J. Hay, W.R. Wadt, *J. Chem. Phys.* 82 (1985) 270.
- [39] W.R. Wadt, P.J. Hay, *J. Chem. Phys.* 82 (1985) 284.
- [40] M.E. Casida, C. Jamorski, K.C. Casida, D.R. Salahub, *J. Chem. Phys.* 108 (1998) 4439.
- [41] V. Barone, M. Cossi, *J. Phys. Chem. A* 102 (1998) 1995.